AIP | Applied Physics Letters

Tuning asymmetry parameter of Fano resonance of spoof surface plasmons by modes coupling

F. Cheng, H. F. Liu, B. H. Li, J. Han, H. Xiao et al.

Citation: Appl. Phys. Lett. **100**, 131110 (2012); doi: 10.1063/1.3698117
View online: http://dx.doi.org/10.1063/1.3698117
View Table of Contents: http://apl.aip.org/resource/1/APPLAB/v100/i13
Published by the American Institute of Physics.

Tuning asymmetry parameter of Fano resonance of spoof surface plasmons by modes coupling

F. Cheng, H. F. Liu, B. H. Li, J. Han, H. Xiao, X. F. Han, C. Z. Gu, and X. G. Qiu[a)]
Beijing National Laboratory for Condensed Matter Physics, Institute of Physics, Chinese Academy of Sciences, P.O. Box 603, Beijing 100190, China

(Received 20 February 2012; accepted 11 March 2012; published online 27 March 2012)

We report a kind of subwavelength, compound hole arrays formed by two nested sub-lattices used to modulate the Fano resonance of spoof surface plasmons (SSPs). Experiments complemented with numerical simulations show that the asymmetry parameter (q) of the Fano line shape can be tuned artificially and continuously: the q value experiences a sign reversal and varies linearly with the variation of hole size. The coupling between different SSP modes of sub-lattices is suggested to be responsible for the tunability of Fano resonance in the compound hole arrays. © *2012 American Institute of Physics*. [http://dx.doi.org/10.1063/1.3698117]

Since the discovery of extraordinary optical transmission (EOT) through subwavelength hole arrays by Ebbesen *et al.*,[1] extensive studies[2–6] have been devoted to investigate the interaction between light and nanostructures. It is generally acknowledged that the excitation of surface plasmon polaritons (SPPs) holds the main physical mechanism responsible for EOT at higher frequencies, ranging from visible[3] to mid-infrared[7] regime. In the past few years, anomalous transmission phenomena in terahertz[8] and microwave[9] regime resembling EOT have also been demonstrated. As we know, due to the extremely low dispersion of SPPs and weakly confined electromagnetic field in the dielectric, metals such as gold and silver behave as perfect electric conductors (PECs) in the far-infrared and terahertz regime which are well below their intrinsic plasma frequencies.[10] Nevertheless, Pendry *et al.* have predicted that by means of appropriate surface patterning, even structures made on PEC can sustain confined surface modes,[11] dubbed spoof surface plasmons (SSPs). The existence of SSPs has been verified by Hibbins *et al.*,[12] extending the SPP-related physics and applications to lower frequencies.[10]

The anomalous transmission spectra show typically asymmetric line shapes, known as Fano resonances.[13] Their steep dispersion is intrinsically sensitive to external changes, which facilitates various applications such as biochemical sensing.[14] Different kinds of nanostructures have been shown to exhibit well-defined Fano line shapes[15] and the asymmetry parameter (q) can be tuned by regulating the external excitations including utilizing symmetry-breaking nanostructures,[16] changing dielectric materials,[17] altering the angle of incidence,[18] and so on.[19,20] However, most of the approaches mentioned above focus in the visible or near-infrared regime where the underneath physics is associated with the excitation of SPP modes. With the SSP-related physics and applications inadequately explored, it is of great interest to extend the asymmetry modulation of Fano resonance to a wider wavelength range. Here a kind of compound hole array formed by two nested sub-lattices was prepared and characterized experimentally to tune the Fano line shape of SSP modes in the far-infrared regime. Numerical simulations using finite element method (FEM) were also carried out, revealing that the coupling between different SSP modes of sub-lattices holds the underlying physical mechanism.

A 100 nm gold film on high-resistance silicon wafer (dielectric constant $\varepsilon = 11.9$) was prepared by magnetron sputtering. To enhance the adhesion of gold to the silicon substrate, a thin layer of 5 nm titanium was deposited on the silicon wafer before the gold sputtering. Subwavelength hole arrays were fabricated on the gold film using ultraviolet photolithography followed by reactive ion etching. The square lattice occupies an area of 7×7 mm^2 with the period $a = 20\,\mu$m, hole size $d = 10\,\mu$m (denoted by 20 – 10) and its scanning electron microscope (SEM) image shown in Fig. 1(a). Our samples are illuminated by linearly polarized infrared radiation with the electric field pointing along the x direction (marked by the red arrow in Fig. 1(a)). The zero-order transmission spectra were obtained using a Fourier transform infrared spectrometer (ABB BOMEM DA8).

Figure 1(e) shows the normalized transmission spectrum of the 20 – 10 lattice. The surface modes can be excited at the metal-dielectric interface, provided that the momentum matching condition is satisfied:

$$\vec{k}_{sp} = \vec{k}_x + \vec{K}^{m,n}, \tag{1}$$

where $\vec{k}_{sp}$ is the surface plasmon wave vector, $\vec{k}_x$ is the in-plane component of incident wave vector, and $\vec{K}^{m,n} = m(2\pi/a)\vec{x} + n(2\pi/b)\vec{y}$ is the reciprocal lattice vector, with a, b being the periods along the x, y directions and m, n integers. Accordingly, the three resonant peaks shown in Fig. 1(e) can be indexed as Si(1,0) mode at 70.9 μm, Si(1,1) mode at 50.3 μm, and Si(2,0) mode at 34.9 μm, respectively. Numerical simulations using FEM have been carried out to further illustrate the resonant features (Fig. 1(i)). Here we treat gold as PEC, i.e., $\varepsilon_{gold} = -\infty$, which is a good approximation for metal in the far infrared regime. Although the defects induced by the micro-fabrication process and the intrinsic polycrystallinity of gold film lead to reduced intensities and broadened line-widths, it can be seen that the main spectral features are well reproduced. Figs. 1(m)–1(o) show

[a)]xgqiu@aphy.iphy.ac.cn.

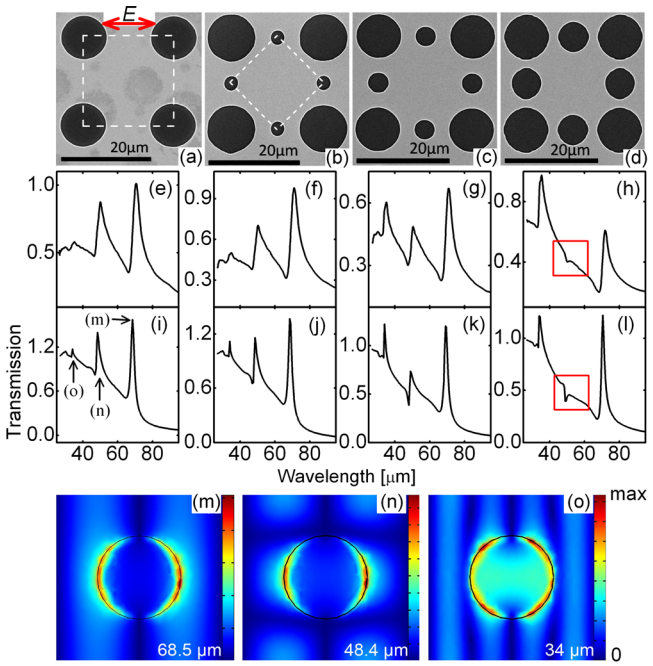

FIG. 1. SEM images of the samples: (a) 20 – 10, (b) 20 – 10 – 3, (c) 20 – 10 – 5, and (d) 20 – 10 – 7, with the same primary hole size ($d = 10\,\mu$m) but different interstitial holes (d_S =0, 3, 5, and 7 μm, respectively). The unit cell of sub-lattices is marked by dashed lines. (e)–(h) Experimental and (i)–(l) simulated transmission spectra of the $20 - 10 - d_S$ lattice. The electric field distributions ($|E|^2$) for the 20 – 10 lattice at 68.5 μm (m), 48.4 μm (n), and 34 μm (o) calculated at 10 nm distance from the interface in the silicon substrate (color legend not the same).

the simulated electric field distributions ($|E|^2$) of the three SSP modes (marked by the arrows in Fig. 1(i)). The nodal patterns at near-field can be seen clearly, which demonstrates the existence of surface confined, SPP-like waves: i.e., the SSP modes are excited at the interface between PEC and the silicon substrate.

The transmission profiles of SSP modes can be characterized by the Fano resonance formula,[21]

$$T = |t|^2 = T_{Bethe}(\lambda) + C\frac{(\lambda - \lambda_{Res} + q\Gamma/2)}{(\lambda - \lambda_{Res})^2 + (\Gamma/2)^2}, \qquad (2)$$

where t is the transmission amplitude, $T_{Bethe}(\lambda)$ is the direct transmission or referred to as Bethe's contribution, C is the non-resonant transmission coefficient, λ_{Res} is the resonant wavelength, q is a dimensionless parameter which describes the asymmetry profile, and Γ is the linewidth, respectively. Generally, the Fano resonance comes from the interference between a continuum radiative waves and a discrete non-radiative state, which has been demonstrated in many physical systems.[14] In the realm of plasmonics, both symmetrical[22,23] and asymmetrical[16,24] structures are shown to exhibit pronounced Fano line shapes. The q value can be influenced by several factors such as geometrical configuration,[25] refractive index of materials,[18] temperature,[20] and so on.

In this letter, an alternative method is proposed to modulate the Fano line shape of SSP modes. We have designed a kind of compound hole arrays by nesting the 20 – 10 lattice with another square lattice with period $a_S = a/\sqrt{2} = 14.1\,\mu$m (marked by the dashed line in Fig. 1(b)) and smaller hole sizes d_S = 3, 5, 7 μm, respectively (denoted as $14.1 - d_S$ with d_S = 3, 5, 7). The coupling effect of different SSP modes of each lattice may be utilized to tune the Fano line shape of the compound hole arrays (denoted by $20 - 10 - d_S$ with the SEM images shown in Figs. 1(b)–1(d)), for which the transmission behavior were studied both experimentally and numerically.

The spectrum of the $20 - 10 - 3$ lattice (Fig. 1(f)) basically resembles that of the 20 – 10 lattice. For the $20 - 10 - 5$ lattice, the intensity of the Si(1,0) and Si(1,1) modes decreases while that of the Si(2,0) mode increases as compared to the $20 - 10 - 3$ lattice (Fig. 1(g)). As d_S increases to 7 μm, the intensity of the Si(2,0) mode increases drastically since larger hole size leads to higher transmission background.[26] However, the magnitude of the Si(1,0) and Si(1,1) modes decrease due to the fact that the SSP modes excited on the 20 – 10 lattice are suppressed by the introduction of the $14.1 - d_S$ lattice. All the transmission features observed in the experiments are well reproduced by the numerical simulations presented in Figs. 1(j)–1(l).

Remarkably, we notice that the Si(1,1) mode of the $20 - 10 - 7$ lattice turns into an anti-resonant dip at 50.3 μm, marked by the red line box in Figs. 1(h) and 1(l). To characterize the asymmetric line shape of the Fano resonance, we fit the Si(1,1) mode using Eq. (2) for the three samples, which are shown in Figs. 2(a)–2(c). For the $20 - 10 - 3$ lattice, the long-wavelength wing of the Si(1,1) mode is relatively steep, in contrast to the flatter short-wavelength wing on the left of the dip at 47 μm and a similar situation is observed for the $20 - 10 - 5$ lattice as well. However, the case of the $20 - 10 - 7$ lattice reverses: the short-wavelength wing becomes steeper as compared with the long-wavelength wing on the right of the dip at 50 μm. In other words, the Fano line shape of the Si(1,1) mode experiences a distinct reversal of the asymmetry, with the q value (labeled in Fig. 2) varying from positive for the $20 - 10 - 5$ lattice to negative for the $20 - 10 - 7$ lattice. Figs. 2(d)–2(f) show the simulated profiles of the Si(1,1) mode and fitting curves for the three samples. Good agreement between experimental and simulated results is obtained.

In order to demonstrate the evolution of the Si(1,1) mode profile in details, we have carried out a series of numerical simulations for the $20 - 10 - d_S$ lattices with d_S ranging from 5 to 8 μm. In Figs. 3(a)–3(e), the results of five lattices and their fitting curves with Eq. (2) are given, from which it can be seen that the asymmetric line shape of the Si(1,1) mode changes gradually with the variation of d_S. The extracted q value follows a good linear relation as d_S increases, evolving from positive (0.81) for the $20 - 10 - 5$ lattice to negative (−1.76) for the $20 - 10 - 8$ lattice and approaches to zero as d_S approximates 6.2 μm, as shown in Fig. 3(f).

The $20 - 10 - d_S$ lattice can actually be considered as the composite of a 20 – 10 lattice nested by a $14.1 - d_S$ one: for each sub-lattice a set of SSP modes can be excited. Not only that, the SSP modes of different sub-lattices can couple together provided that they get close enough, giving rise to the counterintuitive transmission behavior of the compound hole arrays. According to the Bragg coupling relation of Eq. (1), the Si(1,1) mode of the 20 – 10 lattice locates nearly at the same position with the Si(1,0) mode of the $14.1 - d_S$

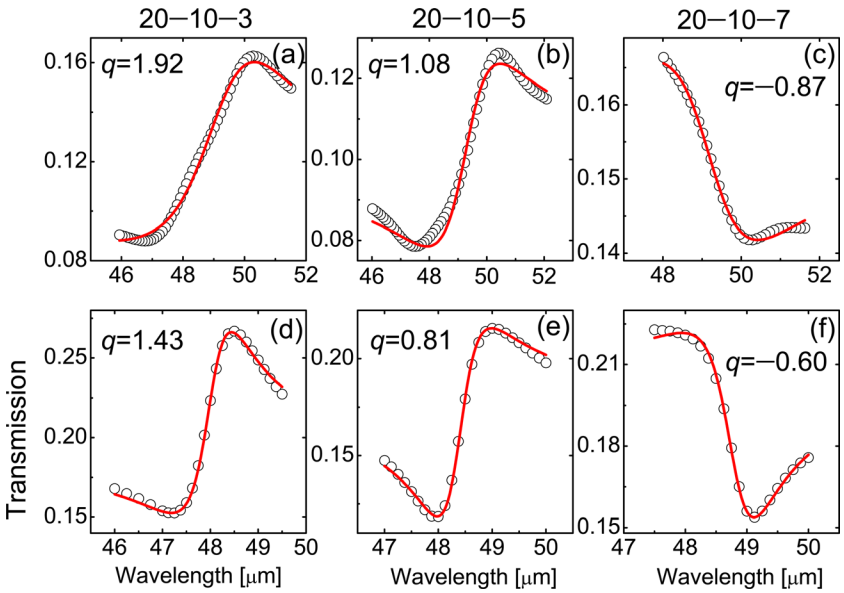

FIG. 2. Experimental (a)–(c) and simulated (d)–(f) transmission spectra (hollow circles) of the Si(1,1) mode for the three compound hole arrays. The solid lines are fitting curves according to Eq. (2). The extracted asymmetry parameter q is labelled for each curve.

lattice. As a consequence, these two adjacent modes may couple coherently with each other, giving rise to constructive or destructive interferences at different wavelengths. On the one hand, the existence of the $14.1-d_S$ lattice can weaken the coherence between 10 μm holes when d_S is large enough, i.e., >5 μm in our case, reducing the excitation probability of SSP modes of the $20-10$ lattice. This is analogous to the scenario[27] where the sign of the asymmetry parameter is determined by the frequency difference between a discrete (dark) state and a plasmonic (bright) mode when the coupling strength of photons to the discrete state is relatively weak. On the other hand, it can be seen in Fig. 4 that the λ_{res} of the Si(1,0) mode for the $14.1-d_S$ lattice red-shifts from 47.9 μm to 48.4 μm as d_S increases from 5 μm to 7.5 μm, since larger hole size increases the cut-off wavelength and analogous red-shift of λ_{res} have been observed in the extraordinary transmission in the visible regime.[3,28] So the Si(1,0) mode of the $14.1-d_S$ lattice passes through the Si(1,1) mode of the $20-10$ lattice ($\lambda_{res}\approx 48.1$ μm, marked by the vertical line in Fig. 4) as d_S increases. As a consequence, the phase of the latter mode reverses[29] and the q value of the Fano resonance for the $20-10-d_S$ lattice flips its sign from positive to negative, as shown in Fig. 2. A symmetric dip emerges as d_S approximates 6.2 μm, near which the cross-over between these two modes takes place.

Since both the spectral position and width of Fano profiles depend sensitively on the geometric parameters or dielectric environment, much interest in plasmonic systems stem from their potential as effective surface plasmon resonance (SPR) sensors. The proposed structure with their highly tunable and sharp Fano resonances may work as SPR substrate for chemical or biological sensing not only in the far infrared but also can be extended to the visible regime where higher sensitivity can be obtained. Meanwhile, the drastic change of the asymmetry parameter from positive to negative can be explored for applications such as optical switches.[14]

In conclusion, for the compound hole arrays reported in this letter, the Fano resonance of SSP modes can be modulated artificially and continuously. The sign of the asymmetry parameter is determined by the relative position of

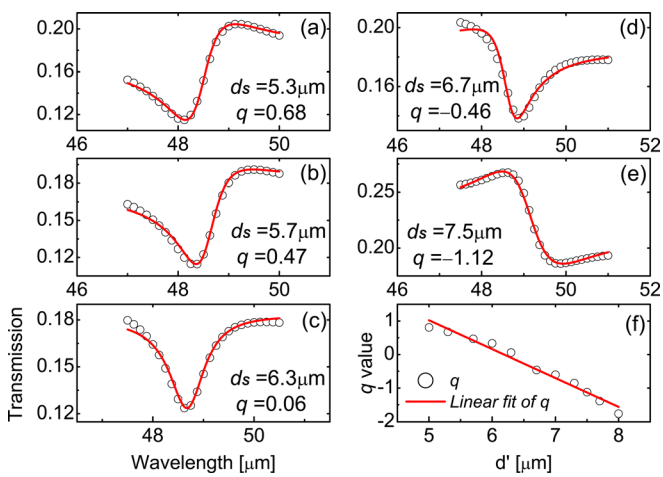

FIG. 3. (a)–(e) The simulated transmission spectra (hollow circles) of the Si(1,1) mode for five $20-10-d_S$ lattices. The solid lines are fitting curves according to Eq. (2). (f) The q value variation and linear fitting as a function of d_S for different $20-10-d_S$ lattices.

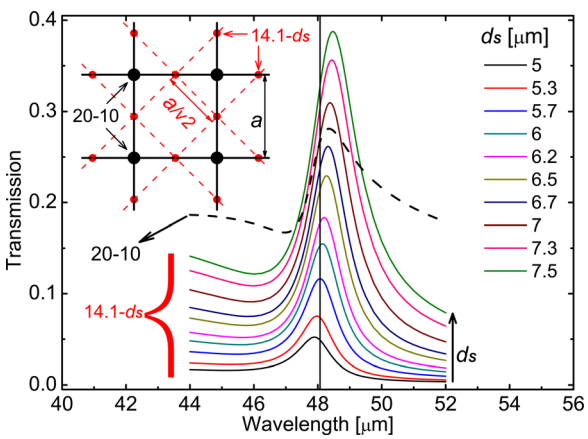

FIG. 4. The simulated Si(1,0) mode of the $14.1-d_S$ lattices ($d_S=5-7.5$ μm, solid) and the Si(1,1) mode of the $10-20$ lattice (dashed). The inset shows the schematic geometric configuration of the compound hole array. The vertical line denotes the λ_{Res} of Si(1,1) mode for the $10-20$ lattice.

coupled SSP modes of sub-lattices. This kind of structures may serve as candidates of building blocks for future metamaterials and hold significant potential in biochemical sensing as well as optical switching applications.

This work is supported by National Basic Research Program of China (No. 2009CB930700, 2009CB929102, 2011CBA00107), National Science Foundation of China (No. 11104335, 91121004) and the Knowledge Innovation Program of CAS (No. KJCX2-EW-W02).

[1]T. W. Ebbesen, H. J. Lezec, H. F. Ghaemi, T. Thio, and P. A. Wolff, Nature (London) **391**, 667 (1998).
[2]E. Popov, M. Neviere, S. Enoch, and R. Reinisch, Phys. Rev. B **62**, 16100 (2000).
[3]L. Martin-Moreno, F. J. Garcia-Vidal, H. J. Lezec, K. M. Pellerin, T. Thio, J. B. Pendry, and T. W. Ebbesen, Phys. Rev. Lett. **86**, 1114 (2001).
[4]W. L. Barnes, W. A. Murray, J. Dintinger, E. Devaux, and T. W. Ebbesen, Phys. Rev. Lett. **92**, 107401 (2004).
[5]X. Fang, Z. Y. Li, Y. B. Long, H. X. Wei, R. J. Liu, J. Y. Ma, M. Kamran, H. Y. Zhao, X. F. Han, B. R. Zhao, and X. G. Qiu, Phys. Rev. Lett. **99**, 066805 (2007).
[6]R. F. Oulton, V. J. Sorger, T. Zentgraf, R.-M. Ma, C. Gladden, L. Dai, G. Bartal, and X. Zhang, Nature(London) **461**, 629 (2009).
[7]Y. H. Ye and J. Y. Zhang, Appl. Phys. Lett. **84**, 2977 (2004).
[8]D. Qu, D. Grischkowsky, and W. Zhang, Opt. Lett. **29**, 896 (2004).
[9]B. Hou, Z. H. Hang, W. Wen, C. T. Chan, and P. Sheng, Appl. Phys. Lett. **89**, 131917 (2006).
[10]C. R. Williams, S. R. Andrews, S. A. Maier, A. I. Fernandez-Dominguez, L. Martin Moreno, and F. J. Garcia-Vidal, Nat. Photon. **2**, 175 (2008).
[11]J. B. Pendry, L. Martn-Moreno, and F. J. Garcia-Vidal, Science **305**, 847 (2004).
[12]A. P. Hibbins, B. R. Evans, and J. R. Sambles, Science **308**, 670 (2005).
[13]U. Fano, Phys. Rev. **124**, 1866 (1961).
[14]B. Luk'yanchuk, N. I. Zheludev, S. A. Maier, N. J. Halas, P. Nordlander, H. Giessen, and C. T. Chong, Nat. Mater. **9**, 707 (2010).
[15]A. E. Miroshnichenko, S. Flach, and Y. S. Kivshar, Rev. Mod. Phys. **82**, 2257 (2010).
[16]F. Hao, Y. Sonnefraud, P. Van Dorpe, S. A. Maier, N. J. Halas, and P. Nordlander, Nano Lett. **8**, 3983 (2008).
[17]A. Christ, O. J. F. Martin, Y. Ekinci, N. A. Gippius, and S. G. Tikhodeev, Nano Lett. **8**, 2171 (2008).
[18]M. V. Rybin, A. B. Khanikaev, M. Inoue, K. B. Samusev, M. J. Steel, G. Yushin, and M. F. Limonov, Phys. Rev. Lett. **103**, 023901 (2009).
[19]M. Kroner, A. O. Govorov, S. Remi, B. Biedermann, S. Seidl, A. Badolato, P. M. Petroff, W. Zhang, R. Barbour, B. D. Gerardot, R. J. Warburton, and K. Karrai, Nature (London) **451**, 311 (2008).
[20]V. A. Fedotov, A. Tsiatmas, J. H. Shi, R. Buckingham, P. de Groot, Y. Chen, S. Wang, and N. I. Zheludev, Opt. Express **18**, 9015 (2010).
[21]C. Genet, M. P. van Exter, and J. P. Woerdman, Opt. Commun. **225**, 331 (2003).
[22]J. A. Fan, C. H. Wu, K. Bao, J. M. Bao, R. Bardhan, N. J. Halas, V. N. Manoharan, P. Nordlander, G. Shvets, and F. Capasso, Science **328**, 1135 (2010).
[23]M. Rahmani, B. Lukiyanchuk, B. Ng, A. Tavakkoli, Y. F. Liew, and M. H. Hong, Opt. Express **19**, 4949 (2011).
[24]X. G. Yin, C. P. Huang, Q. J. Wang, W. X. Huang, L. Zhou, C. Zhang, and Y. Y. Zhu, Opt. Express **19**, 10485 (2011).
[25]B. Pradarutti, G. Torosyan, M. Theuer, and R. Beigang, Appl. Phys. Lett. **97**, 244103 (2010).
[26]H. A. Bethe, Phys. Rev. **66**, 163 (1944).
[27]V. Giannini, Y. Francescato, H. Amrania, C. C. Phillips, and S. A. Maier, Nano Lett. **11**, 2835 (2011).
[28]L. Salomon, F. Grillot, A. V. Zayats, and F. de Fornel, Phys. Rev. Lett. **86**, 1110 (2001).
[29]B. Gallinet and O. J. F. Martin, ACS Nano **5**, 8999 (2011).